Inflammopharmacology (2023) 31:2037–2047
https://doi.org/10.1007/s10787-023-01228-7

Inflammopharmacology

ORIGINAL ARTICLE

Diosmetin alleviates acute lung injury caused by lipopolysaccharide by targeting barrier function

Jiying Xia[1,2] · Junhong Li[1,2] · Mengsheng Deng[3] · Fei Yin[1,2] · Jianhui Liu[1,2] · Jianmin Wang[3]

Received: 23 January 2023 / Accepted: 10 April 2023 / Published online: 19 April 2023

Abstract

Acute lung injury (ALI) is an acute and devastating disease caused by systemic inflammation e.g. patients infected with bacteria and viruses such as SARS-CoV-2 have an unacceptably high mortality rate. It has been well documented that endothelial cell damage and repair play a central role in the pathogenesis of ALI because of its barrier function. Nevertheless, the leading compounds that effectively accelerate endothelial cell repair and improve barrier dysfunction in ALI are largely unknown. In the present study, we found that diosmetin had promising characteristics to inhibit the inflammatory response and accelerate the repair of endothelial cells. Our results indicated that diosmetin accelerated wound healing and barrier repair by improving the expression of the barrier-related proteins, including zonula occludens-l (ZO-1) and occludin, in human umbilical vein endothelial cells (HUVECs) treated with lipopolysaccharide (LPS). Meanwhile, diosmetin administration significantly inhibited inflammatory response by decreasing the content of TNFα and IL-6 in the serum, alleviated lung injury by reducing lung wet/dry (W/D) ratio and histologic score, improved endothelial hyperpermeability by decreasing protein levels and neutrophil infiltration in the bronchoalveolar lavage fluid (BALF) and increasing ZO-1 and occludin expression in the lung tissues of LPS-treated mice. Mechanistically, diosmetin also mediated the expression of Rho A and ROCK1/2 in HUVECs treated with LPS, and fasudil, a Rho A inhibitor remarkably inhibited the role of diosmetin in ZO-1 and occludin proteins. All these findings of this study revealed that diosmetin can be an effective protector of lung injury and the Rho A/ROCK1/2 signal pathway plays a pivotal role in diosmetin accelerating barrier repair in ALI.

Keywords Acute lung injury · Barrier function · Diosmetin · Endothelial cells · Repair

Abbreviations

ALI	Acute lung injury
ARDS	Acute respiratory distress syndrome
BALF	Bronchoalveolar lavage fluid
BHT	Butylated hydroxytoluene
DMEM	Dulbecco's modified Eagle's medium
FBS	Fetal bovine serum
iNOS	Inducible nitric oxide synthase
LPS	Lipopolysaccharide
NF-κB	Nuclear factor kappa B
NO	Nitric oxide
TEAC	Trolox-equivalent antioxidant capacity
TEER	Transepithelial electrical resistance
ZO-1	Zonula occludens-l

Jiying Xia, Junhong Li and Mengsheng Deng have equal contribution to this work.

✉ Jianhui Liu
jhliu@cqut.edu.cn

✉ Jianmin Wang
jmwang@tmmu.edu.cn

[1] Chongqing Key Laboratory of Medicinal Chemistry and Molecular Pharmacology, Chongqing University of Technology, Hongguang Road 69, Ba'nan District, Chongqing 400054, People's Republic of China

[2] College of Pharmacy and Bioengineering, Chongqing University of Technology, Chongqing 400054, People's Republic of China

[3] Research Institute of Surgery, Daping Hospital, Army Medical University, Chongqing 400042, People's Republic of China

Introduction

The global pandemic caused by the severe acute respiratory syndrome coronavirus 2 (SARS-CoV-2) has caused more than 625,938,000 cases, including more than 6,567,000 deaths at the time of writing. Clinical histopathological evidence indicates that patients with SARS-CoV-2 pneumonia

present with severe acute lung injury (ALI) and its more severe form, acute respiratory distress syndrome (ARDS) (Habashi et al. 2021). Currently, according to the pathological and physiological characteristics of ALI/ARDA, corticosteroids, pharmaconutrients, antioxidants, protease inhibitors, ketoconazole, ibuprofen and drugs affecting ventilation, diffusion or perfusion have been used extensively, but the therapeutic effect remains unsatisfactory (Long et al. 2022). Therefore, the development of new drugs for the treatment of ALI/ARDS is in high demand, which could also be useful for the treatment of patients with acute lung injury infected with bacteria and viruses such as SARS-CoV-2.

It has been well documented that most of the patients infected with SARS-CoV-2 showed extensive diffuse alveolar damage and impaired pulmonary perfusion mainly caused by loss of endothelial barrier, lung tissue collapse, severe epithelial injury, and renin-angiotensin system dysfunction (Rello et al. 2020; Beasley 2022). Substantial evidence shows that the increased permeability of the lung microvascular endothelium plays a crucial role in initiating ALI, and the disruption of vascular-endothelial integrity is the major cause of accumulation of protein-rich fluid and neutrophil hyperpermeability in the alveoli. Thus, targeting alveolar endothelial repair may be beneficial to ALI caused by SARS-CoV-2 (Degauque et al. 2021; Jones and Minshall 2022).

In this study, we evaluated the anti-inflammatory activity of diosmetin in a cell model of inflammation treated with lipopolysaccharide (LPS) by determination of nitric oxide (NO) content and determined the influence of diosmetin on the repair and barrier integrity in LPS-treated-human umbilical vein endothelial cells (HUVECs). Meanwhile, we also determined the effects of diosmetin and the Rho A/ROCK1/2 signal pathway on protein expression closely associated with tight junction, including zonula occludens1 (ZO-1) and occludin. In addition, the influence of diosmetin administration in vivo was also evaluated using ALI mice induced by LPS inhalation.

Materials and methods

Materials

ZO-1 (21773-1), Occludin (66378-1), RhoA (10749-1), ROCK1 (21850-1), ROCK2 (21645-1) and β-actin (20536-1) primary antibodies were bought from Proteintech (Wuhan, China). Specific anti-mouse (SC-2386) and anti-rabbit (SC-2374) horseradish peroxidase (HRP)-conjugated second antibodies were obtained from Santa Cruz Biotechnology (Texas, CA, USA). Both mouse TNFα (920) and IL-6 (14206) (ELISA kits were purchased at Huijia Biotechnology (Xiamen, China). Diosmetin (S31450, the purify is over 98%) was bought from Shanghai Yuanye Bio-Technology Co., Ltd (Shanghai, China). Lipopolysaccharides (LPS, ST1470), fluorescein isothiocyanate-dextran (FITC-dextran, 60842-46-8) was obtained from Sigma-Aldrich (St. Louis, MO, USA). Fasudil (Fas, HA-1077) was obtained from Med Chem Express (NJ, USA). GoScript™ Reverse Transcription kit (A2790) and GoTaq qPCR Master Mix (A2800) were purchased from Promega (Madison, WI, USA). ABTS kit (S0121), RIPA buffers (P0013C), BCA protein assay kits (P0012S), the other chemicals were purchased from Beyotime (Shanghai, China).

Cell culture and treatment

Human umbilical vein endothelial cells (HUVECs) and mouse-derived RAW264.7 macrophages were obtained from the China Center for Type Culture Collection, (CCTCC, Wuhan, China) and routinely maintained in high glucose (25 mM) Dulbecco's modified Eagle's medium (DMEM) supplemented with 10% fetal bovine serum (FBS), and 1% penicillin/streptomycin (P/S) at 37 °C in a humidified incubator with 5% CO_2 atmosphere.

Evaluation of the anti-oxidant ability of diosmetin

Anti-oxidative activity of diosmetin was determined by trolox-equivalent antioxidant capacity (TEAC) assay as described before (Usta et al. 2023). Briefly, HUVECs were replaced at 3×10^4/well in 24-well plates and cultured overnight, the cells were pre-incubated with 5, 10, or 20 μM diosmetin or 5 μM butylated hydroxytoluene (BHT, which was a common antioxidant and used as a positive control in this experiment) for 2 h, and then exposed to 500 nM rotenone for 24 h. The cell lysates were collected to assess the antioxidant activity with commercial ABTS kits (S0121, Beyotime, China) in accordance with the suggestions of supplier.

Evaluation of the anti-inflammatory activity of diosmetin

The anti-inflammatory activity of diosmetin was evaluated by determining the nitric oxide (NO) content of the supernatant from LPS-treated macrophages as previously introduced (Liu et al. 2016). Generally, RAW264.7 cells were replaced into 24-well plates (1×10^5 cells/well) and cultured overnight, the cells were pre-treated with indicated concentrations of diosmetin or the same volume of PBS for 2 h, and then exposure to 1 μg/mL LPS for 24 h, the media were gathered to determine NO content using NO test kit from Beyotime (S0021S, Shanghai, China A) in accordance with the suggestions from supplier.

Wound healing test

HUVECs were replaced into 6-well plate at 2×10^5 cells/well and culturing overnight, the monolayer was vertically scratched with a p20 pipette tip, washed with PBS to remove floating cells, and exposed to diosmetin and LPS. The cells were photographed at 0, 24 and 48 h respectively. The invasion index was calculated as the ratio of the closure area to the initial wound as previously described (Zhang et al. 2016): Wound area (%) = (A0 – An)/A0 × 100, where A0 represents the area of original wound area and An represents the remaining area of wound at the point of measurement.

Transendothelial electrical resistance (TEER) measurements

HUVECs were seeded on top of transwell filter chambers on 24-well plates (0.4 µm pore size; Corning, USA), and the medium was refreshed every 2 days. Starting on day 10, the integrity of the cell monolayer was monitored from its TEER as measured using a Millicell® ERS-2 m (Millipore, United States). Typically, when TEER of the monolayers is stable, 5, 10 or 20 µM of diosmetin was added, subsequently, the cells were exposed to 20 µg/mL of LPS for 24 h, and TEER was measured as a function of time at three different locations and calculated using: $TEER_{layer} = (R_{measured} - R_{membrane}) \times$ membrane area, which, $TEER_{layer}$ (Ω cm^2) is the TEER of a cell layer after subtraction of the TEER of the membrane without a cellular layer, $R_{measured}$ (Ω) is the resistance measured of the membrane with a cellular layer and $R_{membrane}$ is the resistance of the membrane measured in absence of a cellular layer.

Measurement of FITC-dextran permeability

To determine the influence of diosmetin on the barrier dysfunction, HUVECs were seeded on top of transwell filter chambers on 24-well plates (0.4 µm pore size; Corning, USA) as previously described (Felix et al. 2021). After reaching the confluence, the cells were preincubated with 5, 10 or 20 µM of diosmetin for 2 h, then 20 µg/mL of LPS was added and continued to incubate for 24 h, the cells were rinsed with PBS and incubated with fresh FBS-free DMEM containing 1 mg/ml FITC-dextran (Sigma-Aldrich, St. Louis, MO, USA) for 45 min. Paracellular flux was assessed by taking 100 µl aliquots from the outer chamber. Fluorescence was measured with a microplate reader (Multiskan FC, Thermo Fisher Scientific, MA, USA) with excitation and emission wavelength at 488 nm and 525 nm, respectively.

Protein extraction and western blot analysis

Mouse lung tissues were homogenized with RIPA lysis buffer (Beyotime) and protease inhibitor cocktail (Sigma). Samples were subjected to 13,000 g 10 min centrifugation at 4 °C. The supernatants were gathered, and the protein concentrations in lysates were measured using the BCA protein assay kit (Beyotime, Shanghai, China). The western blot procedure has been described before (Zhao et al. 2022). In general, equal amounts of protein (20–30 µg each) were separated on a 10% SDS-PAGE and transferred to a PVDF membrane (Immobilon P; Millipore, MA, USA). The blots were blocked for 1 h at room temperature with 5% skimmed milk powder in TBST (20 mM Tris, 150 mM NaCl, 2.7 mM KCl, 0.1% Tween 20, pH 7.4). The membranes were then immunoblotted with ZO-1 and occludin primary antibodies (Proteintech, Wuhan, China) at dilutions of 1:2000 for overnight at 4 °C. Subsequently, blots were washed with TBST three times and incubated for one hour with a HRP-conjugated secondary antibody at 1:10,000 dilution with 5% skimmed milk powder in TBST. Excess antibodies were washed off with TBST, and immunoreactivity was detected using the enhanced chemiluminescence (ECL) western blotting reagent (Millipore). The signal bands have been quantified by densitometry analysis using the Image J software (available from NIH at http://imagej.nih.gov/ij/) after scanning the blotted membrane.

Animal experiments

Male C57BL/6 mice (8–10 weeks) were bought from Tengxin Biotechnology Co. (Chongqing, China), which were allowed ad libitum access to food and water, and rooms were maintained at 25 °C and 50% humidity on a 12-h light/dark cycle. Sixty mice were randomly assigned to six groups: Control, LPS only (10 mg/kg, dissolved in saline), diosmetin (DIO, 5, 10 or 20 mg/kg) + LPS, and dexamethasone (DEX, 5 mg/kg dissolved in saline, which was used as a positive control) + LPS. In brief, diosmetin (5, 10 or 20 mg/kg) and DEX (5 mg/kg) were given intragastrically. Two hours later, 10 mg/kg LPS was administered with intratracheal installation to induce ALI. After 48 h of LPS administration, the animals were euthanized by CO_2 inhalation, and samples of lung tissue, serum, and the broncho-alveolar lavage fluid (BALF) were collected and used for the following experiments. The animal experiments were approved by the Institutional Animal Care and Use Committee at Chongqing Science and Technology Committee (Registration number: 202103) and carried out in accordance with the principles and guidelines of the Chinese Council Animal Care.

Histologic evaluation

Histological examination was conducted using 20 randomly selected fields according to a previously introduced scoring system in a blinded manner (Matute-Bello et al. 2011). Generally, the lung tissues were fixed in freshly prepared 4% polyoxymethylene, dehydrated with ethanol, then embedded in paraffin and cut into 4 μm sections. The sections were stained with haematoxylin and eosin (H&E) double staining, pathological changes based on proteinaceous debris filling the airspace, neutrophils in the alveolar space and the interstitial space, or alveolar septal thickening have been evaluated in LPS-induced ALI mice.

Statistical analysis

Statistical analysis was performed by analysis of variance (ANOVA) and Student *t* test, if applicable, using Graph Pad software (GraphPad Software, La Jolla, CA). The data was presented as means ± SD for a range of experiments. *P* value < 0.05 was considered to be significant.

Results

Anti-inflammatory and antioxidant activity of diosmetin

At present, we firstly determined the cytotoxicity of diosmetin (the chemical structure of diosmetin was shown in Fig. 1a) in RAW264.7 macrophages, MTT assay indicated that diosmetin showed obvious cytotoxicity when the concentrations of diosmetin was over 20 μM ($p < 0.01$, Fig. 1b), but pre-treatment with 5 μM diosmetin slightly increased the cell viability in LPS-treated RAW264.7 macrophages ($p < 0.05$, Fig. 1c).

To assess the anti-inflammatory activity of diosmetin, we determined the NO content in the supernatant of the LPS-treated RAW264.7 macrophages in the presence or absence of diosmetin, the results showed that LPS induced a significant increase of NO content ($p < 0.01$), but diosmetin inhibited the NO content in RAW264.7 macrophages treated with LPS in a dose-dependent manner (Fig. 1d). At the same time, diosmetin dose-dependently decreased the contents of TNF-α (Fig. 1e) and IL-1β (Fig. 1f) in RAW264.7 macrophages challenged by LPS.

In the meantime, we also determined the anti-oxidant ability of diosmetin in rotenone-treated HUVECs with an ABTS assay. Data indicated that incubation with 500 nM for 24 h induced a significant decrease in the total antioxidant capacity of HUVECs, but similar to BHT, a common antioxidant, diosmetin distinctly improved the total antioxidant activity of HUVECs treated with rotenone (Fig. 1g–i).

Diosmetin accelerated the repair of endothelial cells induced by LPS

A large amount of evidence highlights that the lung has a significant capacity to repair and replace damaged cells when confronted with inflammation, and endothelial cells are the primary effectors in initiating tissue repair and the return to homeostasis (Zhao et al. 2017). In this study, the role of diosmetin in tissue repair was evaluated using a scratch wound-healing assay. As shown in Fig. 2a and b, in the presence of 20 μg/mL LPS, the wound healing was obviously inhibited, but diosmetin significantly reduced the wound area compared with control, suggesting that diosmetin may increase the cell spreading in monolayers treated with LPS. We also investigated the effect of diosmetin on barrier dysfunction induced by LPS, after HUVECs were exposed to 20 μg/mL LPS in the presence or absence of diosmetin, TEER and FITC-dextran permeability were measured for the assessment of real-time barrier function. The results showed that diosmetin significantly prevented the decrease of TEER and the increase in FITC-dextran permeability in a dose-dependent manner (Fig. 2c and d). At the same time, data from western blot showed that, although diosmetin treatment had no significant role in the expression of occludin, but was similar to dexamethasone (DEX, which was used as positive control in this study), diosmetin clearly prevented the decrease of ZO-1 protein induced by LPS in HUVECs compared to the control (Fig. 2e–g).

Diosmetin improves barrier dysfunction of endothelial cells via the Rho A/ROCK1 signal pathway

To explore the mechanisms involved in diosmetin improving barrier dysfunction in endothelial cells, we first determined the effect of diosmetin on the expression of Rho A and ROCK1/2 in LPS-treated C57BL/6 mice. The results indicated that LPS clearly caused an increase in Rho A and ROCK1/2, administration of 10 mg/kg LPS for 48 h increased the Rho A, ROCK1, and ROCK2 protein levels approximately 1.7-, 1.3-, and 1.5-folds, respectively, but, pre-treatment with diosmetin greatly reduced the roles of LPS in Rho A and ROCK1/2 proteins in a dose-dependent manner (Fig. 3a and b).

Meanwhile, we found that Rho A and Rock1 were significantly increased and ZO-1 was obviously decreased in LPS-induced HUVECs, but in the presence of 20 μM diosmetin, the roles of LPS in the expression of RhoA, ROCK1 and ZO-1 was distinctly inhibited. In addition, fasudil (FAS), a Rho A kinase inhibitor did not only prevented the role of diosmetin in RhoA and ROCK1/2 expression (Fig. 3e–f), but remarkably attenuated the effects of diosmetin on the expression of barrier-related proteins, including ZO-1 and

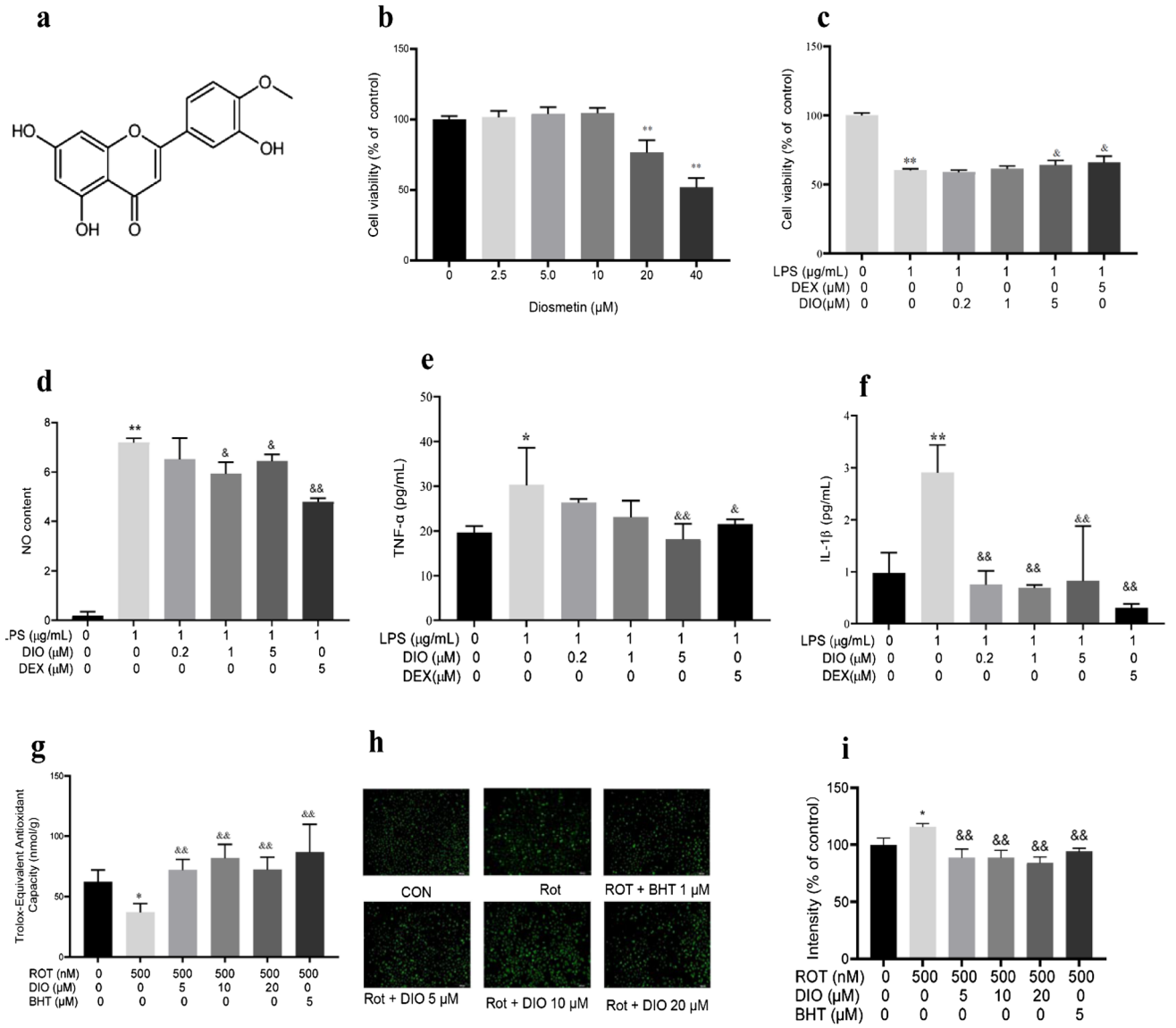

Fig. 1 Anti-inflammatory activity of diosmetin. **a** The chemical structure of diosmetin. **b-c** The cytotoxicity of diosmetin and its effect on cell viability induced by LPS. **d-f** RAW264.7 macrophages were pre-incubated with 0.2, 1 or 5 μM diosmetin (DIO) or 5 μM dexamethasone (DEX) for 2 h and exposed to 1 μg/mL LPS for 24 h. NO content in supernatant, and TNF-α and IL-1β in cell lysates were detected with commercial kits in accordance with the suggestions of supplier. **g** The total antioxidant activity of HUVECs treated with rotenone (ROT) in the presence or absence of diosmetin (DIO) with ABTS kits in accordance with the suggestions from supplier. **h–i** The cells were imaged with fluorescence microscopy (Nikon, Tokyo, Japan), and the fluorescence intensity was determined with a microplate reader (Tecan, Sunrise, USA) with excitation at 485 nm and emission at 530 nm. The data are presented as mean ± SD ($n = 4$), *p < 0.05, **p < 0.01 vs. control, &p < 0.05, &&p < 0.01 vs. The group of LPS alone

occludin (Fig. 3g and h), suggested that the Rho A/ROCK signal pathway could be involved in diosmetin improving barrier dysfunction in LPS-treated HUVECs.

Diosmetin alleviates ALI in mice induced by LPS

As shown in Fig. 4a, LPS induced evidently pathological changes by increasing accumulation of inflammatory cells and alveolar hemorrhage, but similar to dexamethasone (DEX), pre-treatment with diosmetin significantly reduced the effects of LPS in C57BL/6 mice, which was confirmed by the lung injury score (Fig. 4b). Furthermore, diosmetin also attenuated the pulmonary edema by decreasing the W/D ratio in the lung tissues of mice treated with LPS (Fig. 4c). In addition, to assess the anti-inflammatory activity of diosmetin in vivo, serum levels of TNFα and IL-6 were determined using ELISA kits. Our data indicated that pre-treatment with diosmetin substantially decreased the

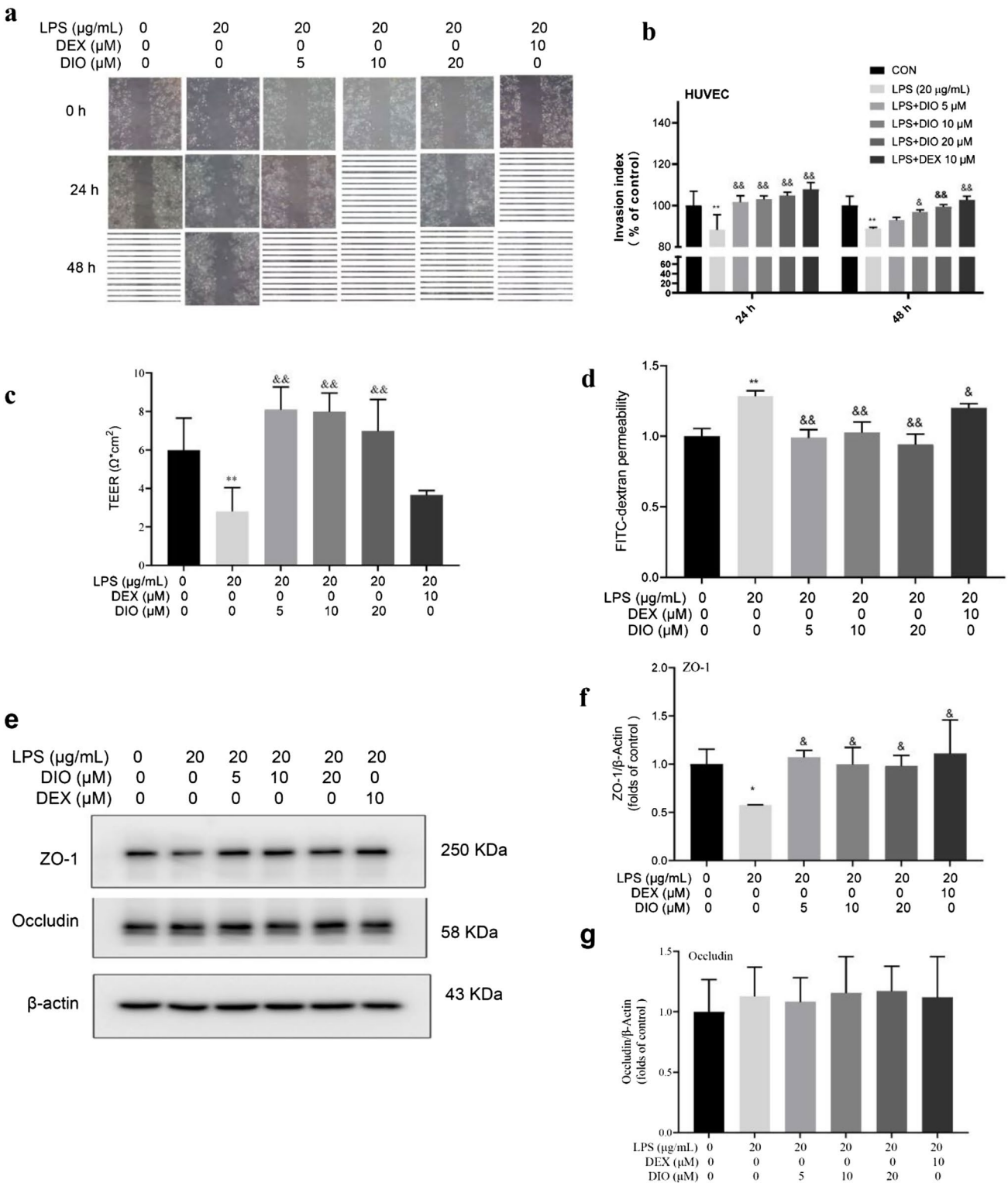

Fig. 2 Diosmetin accelerated endothelial repair in HUEVC treated with LPS. **a** and **b** Microscope images to evaluate wound healing in the scratch assay using a confluent monolayer of HUVECs. Cell migration through the artificial wound was observed after the wounding at 0, 24 and 48 h. Scale bar = 500 μm. **c** and **d** HUVECs were incubated with 20 μg/mL LPS in the presence or absence of indicated concentrations of diosmetin (DIO), and then TEER (**c**) and FITC-dextran infiltration (**d**) were evaluated as introduced in the Methods. **e–g** HUVECs were pre-treated with 5, 10 or 20 μM diosmetin (DIO) for 2 h and exposed to 20 μg/mL LPS for 24 h, the content of ZO-1 and occludin proteins were determined with western blot. The data are presented as mean ± SD (n = 6 for TEER and FITC-dextran assay and n = 3 for western blot), *p < 0.05, **p < 0.01 vs. control, and &p < 0.05, &&p < 0.01 vs. The group of LPS alone

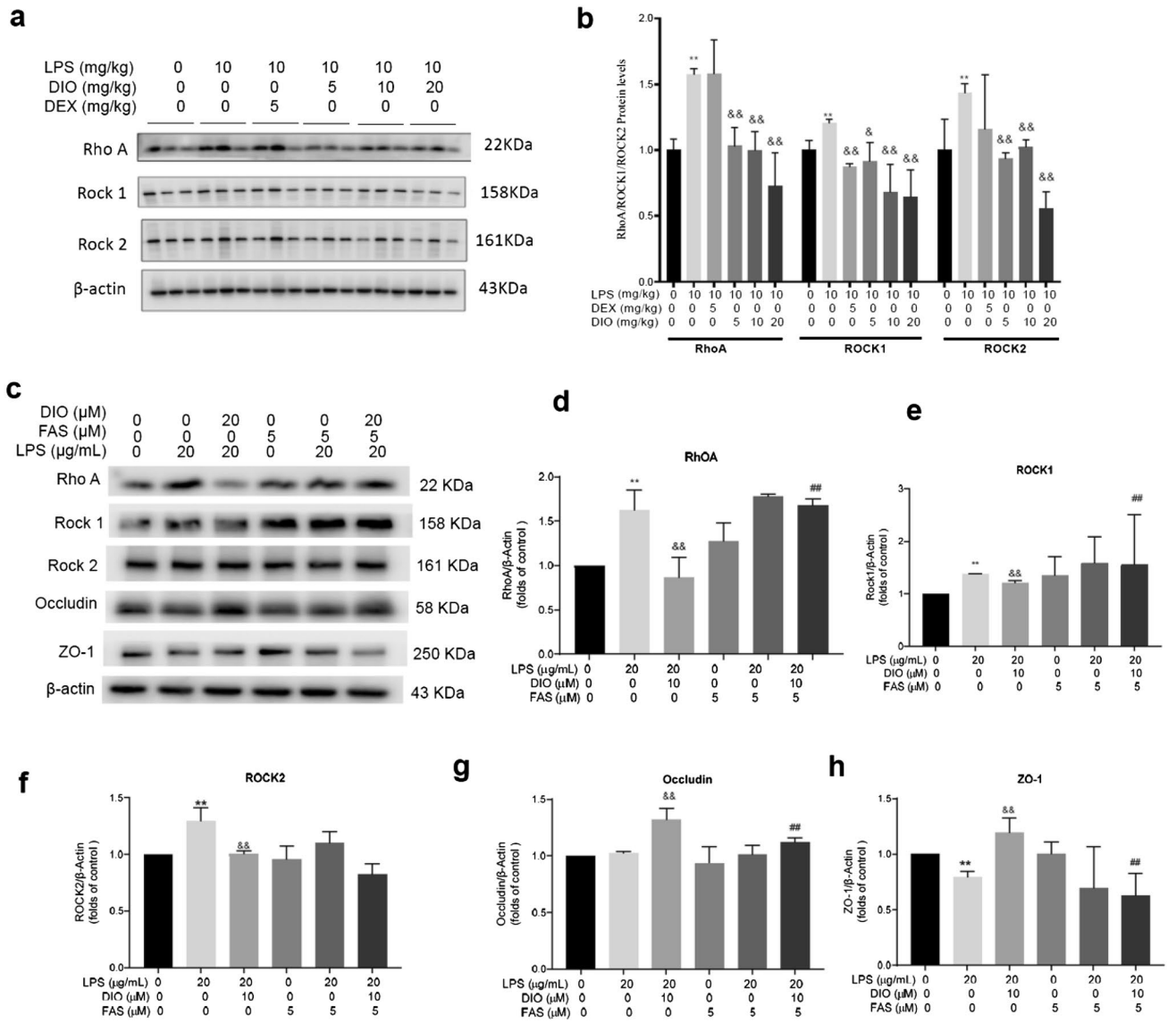

Fig. 3 Diosmetin regulated ZO-1 and occludin expression via the Rho A/ROCK1/2 signal pathway. **a–b** The mice were pre-treated with 5, 10, or 20 mg/kg diosmetin (DIO) for 2 h before LPS was intratracheally instilled, after 48 h of exposure to LPS (10 mg/kg), the mice were euthanized, the and lung tissues were collected. The protein levels of Rho A, Rock1, ROCK2, occludin, ZO-1, and β-actin were detected by western blot. **c–h** After HUVECs were replaced into 6-well/plate and cultured overnight, the cells were preincubated with 5 μM fasduil (FAS) for 1 h, and then exposed to 5, 10 or 10 μM of diosmetin (DIO) for 24 h with 20 μg/mL LPS, the protein levels of Rho A, Rock1, ROCK2, occludin, ZO-1, and β-actin were detected by western blot. The data are presented as mean ± SD (n = 3). *$p < 0.05$, **$p < 0.01$ vs. control, and &$p < 0.05$, &&$p < 0.01$ vs. the group of LPS alone, and ##$p < 0.01$ vs. The group of LPS plus diosmetin

levels of TNFα (Fig. 4d) and IL-6 (Fig. 4e) in the serum of LPS-treated mice.

Diosmetin ameliorates barrier dysfunction in LPS-treated mice

To evaluate the effect of LPS and diosmetin on alveolar barrier permeability, we measured the exuded protein, the total number of cells, the WBC, and the NEUT in the BALF, the results showed that LPS induced an evident barrier dysfunction by increasing the content of the exuded protein (Fig. 5a), the WBC (Fig. 5b), the NEUT (Fig. 5c) and the total number of cells (Fig. 5d) in the BALF, whereas pretreatment with diosmetin has significantly prevented protein permeability and the increase of these cells induced by LPS.

To further investigate the mechanisms involved in diosmetin improving alveolar barrier permeability, we determined the proteins associated with barrier function, including ZO-1 and occludin in the lungs of ALI mice. Western blot results indicated that diosmetin clearly prevented the

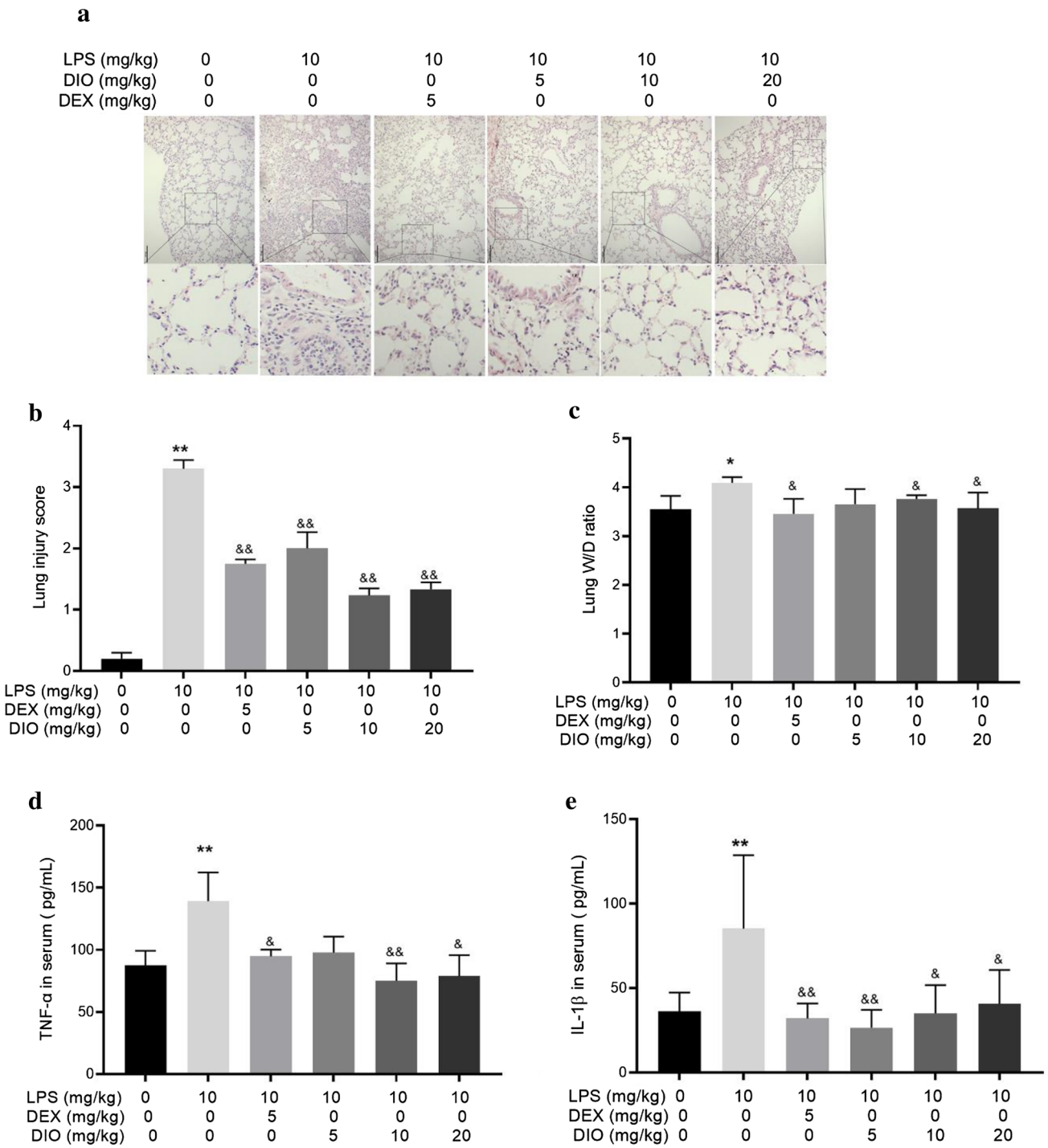

Fig. 4 Diosmetin alleviated ALI in C57BL/6 mice induced by LPS. The mice were pre-treated intragastrically with 5, 10, or 20 mg/kg diosmetin (DIO) for 2 h before 10 mg/kg LPS was intratracheally instilled in order to establish an ALI model, after 48 h of LPS administration, the animals were euthanized by CO_2 inhalation, and lung tissue samples were collected and evaluated with H&E staining (**a**), Lung W/D ratio was measured (**b**), lung injury score was assessed (**c**), and the inflammatory cytokines, including TNFα (**d**) and IL-6 (**e**) were determined using ELISA kits. The data are presented as mean ± SD (n = 4 for ELISA and n = 10 for histological evaluation), *p < 0.05, **p < 0.01 vs. control, and &p < 0.05, &&p < 0.01 vs. The group of LPS alone

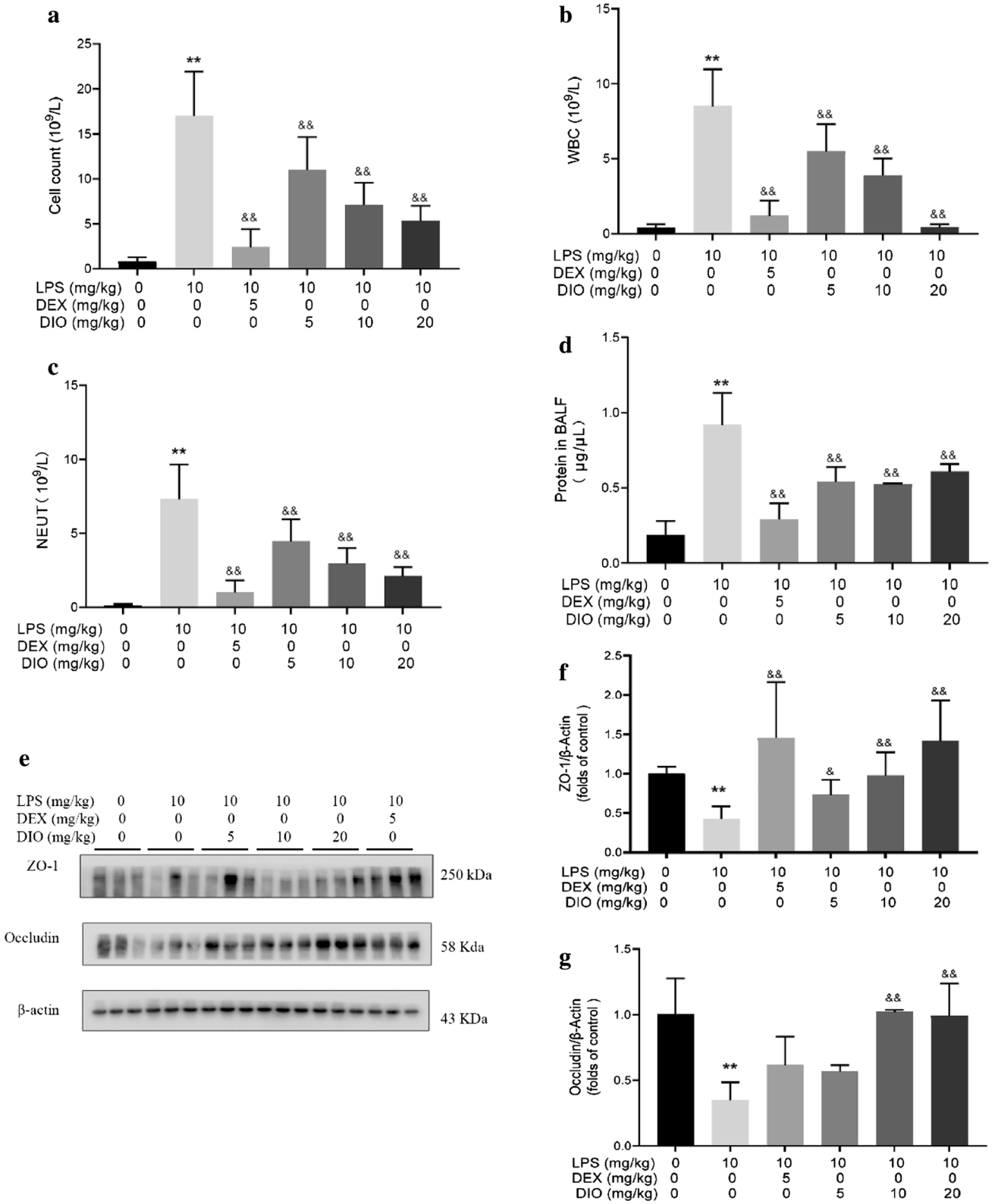

Fig. 5 Diosmetin improved lung barrier dysfunction in LPS-induced ALI mice. The total cell count (**a**), WBC (**b**), and NEUT(**c**) in BALF were determined with a hemocytometer, the protein content in the BALF (**d**) was determined with BCA kits. Meanwhile, the protein levels of ZO-1 and occludin were detected with western blot (**e–g**). The data are expressed as mean ± SD (n = 3 for western blot, and n = 10 for cell count and protein content). **p < 0.01 vs. control, and &p < 0.05, &&p < 0.01 vs. The group of LPS alone

reduction of ZO-1 and occludin proteins in the lung tissues of mice induced by LPS (Fig. 5e–g).

Discussion

It has been well documented that viral infection and the following adaptive and innate host response lead to a severely damaged alveolar epi/endothelial barrier, and the re-epithelialization and re-sealing of endothelial cells is considered as a critical step in restoring normal conditions of gas exchange in the lung (Matthay et al. 1993; Herrero et al. 2018). Currently, diosmetin was examined to demonstrate significant anti-inflammatory activity, accelerate wound healing, and improve endothelial resistance and FITC-dextran permeability by increasing ZO-1 expression, one of the key molecules associated with barrier function, suggesting that diosmetin may be a promising compound that is useful in improving barrier dysfunction of ALI.

The accumulation of evidence highlights that ALI is characterized by extensive neutrophil infiltration, inflammatory cytokine release, increased capillary permeability, and edema (Gorovoy et al. 2009). Here, diosmetin was found to reduce the content of inflammatory factors, including TNFα and IL-6 in serum, to reduce lung injury and pulmonary edema in LPS-induced C57BL/6 mice. In addition, diosmetin administration distinctly prevented the rise of lung W/D ratio, the infiltration of proteins and neutrophils in LPS-induced ALI. In parallel, diosmetin also increased the expression of barrier-related proteins in the lung tissue of mice treated with LPS. All these results indicate that diosmetin may be beneficial in reducing pulmonary permeability in ALI.

A growing body of evidence indicates that RhoA plays a crucial role in inducing contraction-driven endothelial hyperpermeability by stimulating cell progression, migration and invasion, and by acting through ROCK1 and ROCK2 effecting proteins (Carbajal and Schaeffer 1999). And, several studies had addressed the role of RhoA in endothelial barrier function, which could be activated by thrombin and vascular endothelial growth factor (VEGF) and caused a disrupted barrier due to the activation of ROCK1/2 (van Nieuw Amerongen et al. 2003, 2008; Wang et al. 2010). In this study, we found that in addition to increasing the content of protein-related barrier, diosmetin considerably reduced the roles of LPS in the expression of Rho A and ROCK1/2, but in the presence of fasudil, an inhibitor of Rho A, the effects of diosmetin on the expression of ZO-1 and occludin were obviously inhibited, suggesting that the Rho A/ROCK signal pathway played an important role in diosmetin regulating the levels of ZO-1 and occludin proteins.

Diosmetin is abundant in citrus fruits and has long been noticed due to its favorable pharmacological activities including antibacterial, antioxidative stress, and anti-inflammatory property (Shen et al. 2016; Lee et al. 2020). The traditional advantages of citrus fruits attributed to their content of flavonoids and polyphenols are its actions on the improvement of glycolipid metabolic disorders (Sharma et al. 2019). But recently, diosmetin has been shown to inhibit the activation of NLRP3 inflammasome in LPS-induced ALI (Liu et al. 2018), and prevent acute hepatic failure in endotoxin-induced mice and cerulenin-induced acute pancreatitis by attenuating the secretion of TNFα, IL-1β and IL-6, the activation of nuclear factor kappa B (NF-κB), and the expression of inducible nitric oxide synthase (iNOS) (Yu et al. 2014; Yang et al. 2017). All these data suggest that diosmetin has extensive activities.

Overall, although a variety of natural products including diosmetin have been studied to treat ALI as regards their anti-inflammatory and lung protective effects (He et al. 2021), but the role of diosmetin in the barrier dysfunction of ALI remains uncertain. Accumulating evidence suggests that a severe endothelial injury appears at an early stage of diffuse alveolar damage, which is characterized by endothelial dysfunction and loss of pulmonary perfusion caused by the endothelial barrier (Jones and Minshall 2022). The results of this study demonstrated that diosmetin was effectively in protecting ALI by regulating the expression of protein-related barrier in vitro and in vivo, which provided valuable evidence for the potential application of diosmetin in the treatment of ALI.

Acknowledgements This work was supported by Army medical project (NO. ALJ18J001), and the Scientific and Technological Research Program of Chongqing Municipal Education Commission (KJZD-K202101102).

Author contributions XJY, LJH and DMS performed the experiments; YF analyzed the data. LJH and WJM were the major contributors to design the research and writing the manuscript. All authors read and approved the final manuscript. All data were generated in-house, and no paper mill was used. All authors agree to be accountable for all aspects of work ensuring integrity and accuracy.

Funding Army medical project (ALJ18J001).

Availability of data and materials The data and materials for this study are available from the corresponding author upon reasonable request.

Declarations

Conflict of interest The authors declare that they do not have any conflict of interest.

References

Beasley MB (2022) Acute lung injury-from cannabis to COVID. Mod Pathol 35(Suppl 1):1–7. https://doi.org/10.1038/s41379-021-00915-6

Carbajal JM, Schaeffer RC Jr (1999) RhoA inactivation enhances endothelial barrier function. Am J Physiol 277(5 Pt 1):C955-964. https://doi.org/10.1152/ajpcell.1999.277.5.C955

Degauque N, Haziot A, Brouard S, Mooney N (2021) Endothelial cell, myeloid, and adaptive immune responses in SARS-CoV-2 infection. FASEB J 35(5):e21577. https://doi.org/10.1096/fj.202100024R

Felix K, Tobias S, Jan H, Nicolas S, Michael M (2021) Measurements of transepithelial electrical resistance (TEER) are affected by junctional length in immature epithelial monolayers. Histochem Cell Biol 156(6):609–616. https://doi.org/10.1007/s00418-021-02026-4

Gorovoy M, Han J, Pan H, Welch E, Neamu R, Jia Z, Predescu D, Vogel S, Minshall R, Ye R, Malik A, Voyno-Yasenetskaya T (2009) LIM kinase 1 promotes endothelial barrier disruption and neutrophil infiltration in mouse lungs. Circulation Res 105(6):549–556. https://doi.org/10.1161/circresaha.109.195883

Habashi NM, Camporota L, Gatto LA, Nieman G (2021) Functional pathophysiology of SARS-CoV-2-induced acute lung injury and clinical implications. J Appl Physiol 130(3):877–891. https://doi.org/10.1152/japplphysiol.00742.2020

He YQ, Zhou CC, Yu LY, Wang L, Deng JL, Tao YL, Zhang F, Chen WS (2021) Natural product derived phytochemicals in managing acute lung injury by multiple mechanisms. Pharmacol Res 163:105224. https://doi.org/10.1016/j.phrs.2020.105224

Herrero R, Sanchez G, Lorente JA (2018) New insights into the mechanisms of pulmonary edema in acute lung injury. Ann Transl Med 6(2):32. https://doi.org/10.21037/atm.2017.12.18

Jones JH, Minshall RD (2022) Endothelial transcytosis in acute lung injury: emerging mechanisms and therapeutic approaches. Front Physiol 13:828093. https://doi.org/10.3389/fphys.2022.828093

Lee H, Sung J, Kim Y, Jeong HS, Lee J (2020) Inhibitory effect of diosmetin on inflammation and lipolysis in coculture of adipocytes and macrophages. J Food Biochem 44(7):e13261. https://doi.org/10.1111/jfbc.13261

Liu Q, Li D, Wang A, Dong Z, Yin S, Zhang Q, Ye Y, Li L, Lin L (2016) Nitric oxide inhibitory xanthones from the pericarps of *Garcinia mangostana*. Phytochemistry 131:115–123. https://doi.org/10.1016/j.phytochem.2016.08.007

Liu Q, Ci X, Wen Z, Peng L (2018) Diosmetin alleviates lipopolysaccharide-induced acute lung injury through activating the Nrf2 pathway and inhibiting the NLRP3 inflammasome. Biomol Ther (seoul) 26(2):157–166. https://doi.org/10.4062/biomolther.2016.234

Long ME, Mallampalli RK, Horowitz JC (2022) Pathogenesis of pneumonia and acute lung injury. Clin Sci (lond) 136(10):747–769. https://doi.org/10.1042/CS20210879

Matthay MA, Folkesson HG, Campagna A, Kheradmand F (1993) Alveolar epithelial barrier and acute lung injury. New Horiz 1(4):613–622. https://doi.org/10.1007/978-3-662-13455-9_17

Matute-Bello G, Downey G, Moore BB, Groshong SD, Matthay MA, Slutsky AS, Kuebler WM, Acute Lung Injury in Animals Study, G (2011) An official American Thoracic Society workshop report: features and measurements of experimental acute lung injury in animals. Am J Respir Cell Mol Biol 44(5):725–738. https://doi.org/10.1165/rcmb.2009-0210ST

Rello J, Storti E, Belliato M, Serrano R (2020) Clinical phenotypes of SARS-CoV-2: implications for clinicians and researchers. Eur Respir J. https://doi.org/10.1183/13993003.01028-2020

Sharma K, Adhikari D, Kim HJ, Oh SH, Oak MH, Yi E (2019) Citrus junos fruit extract facilitates anti-adipogenic activity of *Garcinia cambogia* extract in 3T3-L1 adipocytes by reducing oxidative stress. J Nanosci Nanotechnol 19(2):915–921. https://doi.org/10.1166/jnn.2019.15915

Shen Z, Shao J, Dai J, Lin Y, Yang X, Ma J, He Q, Yang B, Yao K, Luo P (2016) Diosmetin protects against retinal injury via reduction of DNA damage and oxidative stress. Toxicol Rep 3:78–86. https://doi.org/10.1016/j.toxrep.2015.12.004

Usta M, Semerci T, Aydinhan M, Guder A, Koseoglu MH (2023) Biological variations of seven clinical chemistry analytes and trolox equivalent antioxidant capacity within salivary constituents. Clin Lab. https://doi.org/10.7754/Clin.Lab.2022.220532

van Nieuw Amerongen GP, Koolwijk P, Versteilen A, van Hinsbergh VW (2003) Involvement of RhoA/Rho kinase signaling in VEGF-induced endothelial cell migration and angiogenesis in vitro. Arterioscler Thromb Vasc Biol 23(2):211–217. https://doi.org/10.1161/01.ATV.0000054198.68894.88

van Nieuw Amerongen GP, Musters RJ, Eringa EC, Sipkema P, van Hinsbergh VW (2008) Thrombin-induced endothelial barrier disruption in intact microvessels: role of RhoA/Rho kinase-myosin phosphatase axis. Am J Physiol Cell Physiol 294(5):C1234-1241. https://doi.org/10.1152/ajpcell.00551.2007

Wang Z, Ginnan R, Abdullaev IF, Trebak M, Vincent PA, Singer HA (2010) Calcium/Calmodulin-dependent protein kinase II delta 6 (CaMKIIdelta6) and RhoA involvement in thrombin-induced endothelial barrier dysfunction. J Biol Chem 285(28):21303–21312. https://doi.org/10.1074/jbc.M110.120790

Yang Y, Gong XB, Huang LG, Wang ZX, Wan RZ, Zhang P, Zhang QY, Chen Z, Zhang BS (2017) Diosmetin exerts anti-oxidative, anti-inflammatory and anti-apoptotic effects to protect against endotoxin-induced acute hepatic failure in mice. Oncotarget 8(19):30723–30733. https://doi.org/10.18632/oncotarget.15413

Yu G, Wan R, Yin G, Xiong J, Hu Y, Xing M, Cang X, Fan Y, Xiao W, Qiu L, Wang X, Hu G (2014) Diosmetin ameliorates the severity of cerulein-induced acute pancreatitis in mice by inhibiting the activation of the nuclear factor-kappaB. Int J Clin Exp Pathol 7(5):2133–2142

Zhang J, Chen C, Hu B, Niu X, Liu X, Zhang G, Zhang C, Li Q, Wang Y (2016) Exosomes derived from human endothelial progenitor cells accelerate cutaneous wound healing by promoting angiogenesis through Erk1/2 signaling. Int J Biol Sci 12(12):1472–1487. https://doi.org/10.7150/ijbs.15514

Zhao Y, Ridge K, Zhao J (2017) Acute lung injury, repair, and remodeling: pulmonary endothelial and epithelial biology. Mediators Inflamm 2017:9081521. https://doi.org/10.1155/2017/9081521

Zhao WJ, Bian YP, Wang QH, Yin F, Yin L, Zhang YL, Liu JH (2022) Blueberry-derived exosomes-like nanoparticles ameliorate nonalcoholic fatty liver disease by attenuating mitochondrial oxidative stress. Acta Pharmacol Sin 43(3):645–658. https://doi.org/10.1038/s41401-021-00681-w